

Fuzzy measurements and coarse graining in quantum many-body systems

Carlos Pineda,^{1,*} David Davalos,¹ Carlos Viviescas,² and Antonio Rosado¹

¹*Instituto de Física, Universidad Nacional Autónoma de México, Ciudad de México 01000, México*

²*Departamento de Física, Universidad Nacional de Colombia, Carrera 30 No. 45-03, Bogotá D.C., Colombia*

We provide a framework to construct fuzzy and coarse grained quantum states of many-body systems using quantum maps that account for limitations in the resolution of real measurement devices. The first set of maps handles particle-indexing errors, while the second deals with the effects of detectors that can only resolve a fraction of the systems particles. Fuzzy and coarse grained maps are simply related via a partial trace, what allow us to concentrate on the properties of the former. We fully characterize its symmetries and in turn identify its invariant spaces, and show that the volume of the tomographically accessible states decreases at a double exponential rate, indicating the inability to read and use information of a many-body quantum system. We apply these maps to the study of entanglement generation and propagation in a spin-1/2 XX-chain.

Introduction.— Nowadays, quantum many-body systems can be manipulated at the single particle level with high precision [1], yet, like with all systems in nature, limitations in measurements set the boundaries of what we can learn about them. Not surprisingly, measurement has had a prominent role in quantum mechanics since its foundation, being a topic of intense research up to this date [2, 3], but not always advancing at the same pace of the control that has been gained over quantum systems. At this stage, for quantum many-body systems, in particular, a theory of imperfect detection would help broadening our understanding of fundamental aspects of these systems.

Quantum many-body systems can be classified into two families: naturally occurring systems, e.g. medium and large molecules, polymers; and crafted ones, such as ion chains, neutral atoms in lattices, etc. In the first family, groups of particles are often treated collectively as an effective particle, either because the measurement device is not sensible enough to resolve all degrees of freedom in the system, or because only a few of those degrees of freedom are of relevance for the system property being studied. Such scenario corresponds to a *coarse graining* (CG) view of the system, as it is commonly found in nuclear magnetic resonance. In the second family, single particles can be resolved, however, there is always a probability of misidentifying them. We shall call this kind of imperfect detection a *fuzzy measurement* (FM).

Both imperfect measurements and CG have been studied before in different settings within the framework of quantum mechanics. Peres considered imperfect measurements when assessing the consequences of having an experimental uncertainty in the eigenvalue measurement similar or larger to the difference between consecutive eigenvalues [4]. In this context, projective measurements were generalized to positive operator value measurements, which allowed for a gentle effect on the measured system [5] and for other schemes, which were referred to as unsharp, weak and fuzzy measurements [6–8]. The information theoretical background of statistically coarse grained descriptions, obtained through stochastic

maps, and its applicability to quantum mechanics, in a single body setting, is discussed in [9]. In [10, 11] it has been argued that classical features emerge from coarse grained descriptions of quantum systems, and more recently, a based on measurement approach to CG was proposed in [12, 13]. These progress, notwithstanding, an inclusive framework for a multipartite system, that could systematically address the implications of studying quantum many-body systems using imperfect measurements, is still missing.

In this letter we construct and exploit a framework to study both FM and CG in quantum many-body systems. We formalized both concepts in the language of quantum maps and apply them to the study of entanglement waves, as an illustrative example. As we show, both concepts are deeply related, so we provide a mathematical characterization of them, identifying their symmetries, spectrum and invariant spaces. To conclude, we put special attention to the maps action on the state space, considering their contraction properties, and how Uhlmann’s theorem can be applied to identify some physical consequences, such as the reduction of observable entanglement within the system.

Fuzzy measurements.— Suppose a measurement of the observable $A \otimes B$ in a two particle system is wanted. Yet, with probability $1 - p$, the measurement apparatus mistakes the particles, so instead, sometimes, a measurement of $B \otimes A$ is done. Hence, if ρ is the state of the system, the outcome of this FM is

$$p \operatorname{Tr} \rho A \otimes B + (1 - p) \operatorname{Tr} \rho B \otimes A = \langle A \otimes B \rangle_{\mathcal{F}_{2p}[\rho]}. \quad (1)$$

The effective tomographically accessible state of the two-particle system is $\mathcal{F}_{2p}[\rho] = p\rho + (1 - p)S_{01}[\rho]$. Here, $\langle \cdot \rangle_{\varrho}$ denotes the expected value with respect to ϱ , and the brackets in front of a unitary operator denote its natural action on density matrices, e.g. $S_{ij}[\rho] = S_{ij}\rho S_{ij}^{\dagger}$ is the application of the swap gate with respect to particles i and j to the system state. The above reasoning can be followed in the case of an n -body system. If the measurement device wrongly identifies the particles with

probability $p_P \geq 0$, according to permutation P , the outcome of the FM of operator M is $\text{Tr}(M\mathcal{F}[\rho])$, with

$$\mathcal{F}[\rho] = \sum_{P \in \mathcal{S}} p_P P[\rho], \quad (2)$$

and \mathcal{S} a subset of the symmetric group of n particles, and $\sum_{P \in \mathcal{S}} p_P = 1$. We regard Eq. (2) as the most general form of the FM channel. We consider some particular examples below.

Quite generally during a measurement two-body errors are more likely to occur than higher order ones. Accounting just for these, the effective tomographically accessible state is

$$\mathcal{F}_{2b}[\rho] = p\rho + (1-p) \sum_{i,j} p_{ij} S_{ij}[\rho], \quad (3)$$

with \mathcal{S} containing only swaps. A relevant related case is a periodic one-dimensional chain in which errors between adjacent particles are the only ones taken into account. In this case

$$\mathcal{F}_{1d}[\rho] = p\rho + (1-p) \sum_i p_i S_{i,i+1}[\rho] \quad (4)$$

with \mathcal{S} consisting of neighboring exchanges. Similar considerations can be done for two-dimensional systems, more refined proposals, e.g. a swap probability that decays with distance between i and j , or a particular experimental setup.

Coarse graining.— Consider now the situation in which the measurement device is unable to resolve the fine details of the whole system, and is forced to capture effective reduced states of randomly chosen subsets of the system. Two processes characterize such an apparatus: The choice of random subsets and the reduction to a representative state as a result of a partial trace of the subset, accounting for the discarded information of the inaccessible parts and providing a *coarse grained* picture of the system state. This is clearly illustrated in the simple case of a two-particle system. The expected value of the single particle observable M measured by an apparatus that with probability p detects the first particle and with $1-p$ the second one is $\text{Tr}(M\rho_{\text{eff}})$, with the effective single particle state $\rho_{\text{eff}} = \text{Tr}_1 \mathcal{F}_{2p}[\rho]$.

The same procedure can be applied to systems with more than two particles. Assume a detector is able to measure only N particles at a time, picking each one of them randomly from subsets of m_k particles, with $k = 1, \dots, N$. The effective N particle state is given by

$$\rho_{\text{eff}} = \left(\bigotimes_k \mathcal{C}_{m_k} \right) [\rho], \quad \mathcal{C}_m[\rho] = \frac{1}{m} \text{Tr}_{\bar{1}} \sum_i S_{1,i}[\rho], \quad (5)$$

where the trace is over all elements but the first particle. Notice that the channel is the composition of a FM and a partial trace, a consequence of the linearity of the trace

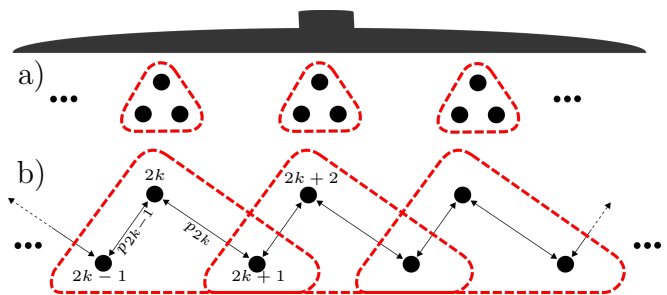


FIG. 1. CG schemes. (a) The detector is grouping sets of $m = 3$ particles into one, see eq. (12). (b) The detector measures even particles with larger probability than odd ones, but sometimes it mistakes them for one of their neighbors, see eq. (6).

and the group properties of permutations; see the Supplementary Material for details. The case $m_k = m = 3$ is depicted in fig. 1(a).

Motivated by a different physical feasible situation, we examine a second coarse grained measurement with its corresponding FM. Consider a chain of particles that alternate, such that the even ones are closer to the detector than the odd ones, see fig. 1(b) for an example. Assume that with probability p the measurement device measures the even particles, but with a position dependent probability one of its odd-labeled neighbors is detected. The channel associated with such measurement is

$$p \text{Tr}_{\text{odd}} \rho + (1-p) \text{Tr}_{\text{odd}} \sum_i p_i S_{i,i+1}[\rho] = \text{Tr}_{\text{odd}} \mathcal{F}_{1d}[\rho]. \quad (6)$$

Single particle observables of, say, particle $2i$ are evaluated with respect to the effective density matrix $[1 + p(p_{2i-1} + p_{2i})]\rho_{2i} + pp_{2i-1}\rho_{2i-1} + pp_{2i}\rho_{2i+1}$, where ρ_i is the reduced density matrix for particle i . Two particle observables, say of particles $2i$ and $2j$, are calculated with a density matrix, with coefficients of order zero in $1-p$ of $\rho_{2i,2j}$, and other contributions of order one, of $\rho_{2i\pm 1,2j}$ and $\rho_{2i,2j\pm 1}$.

The above examples show how to construct reduced quantum states using quantum maps motivated by probabilistically chosen subsystems that become more relevant to the measurement of certain observables, when the interplay between the physical system and the measurement apparatus is taken into account. Generalizations, to build reduced quantum states using quantum maps for more general models that allowed for the simultaneous interchange of a greater number of particles are possible. An encompassing scheme for CG maps is

$$\mathcal{C}[\rho] = \text{Tr}_{\tau} \sum_{P \in \mathcal{S}} p_P P \rho P^\dagger = \text{Tr}_{\tau} \mathcal{F}[\rho], \quad (7)$$

where τ denotes the part of the system that is traced.

Fuzzy and coarse grained entanglement waves.—We now consider the recently achieved observation of a single spin impurity dynamics [14] and spin-entanglement wave

propagation [15] in one dimensional Bose-Hubbard chains at the level of single-atom-resolve detection [16, 17], to illustrate the use of the proposed maps.

The dynamics of a single spin impurity in a one dimensional homogeneous spin-1/2 XX -chain is generated by the Hamiltonian $\hat{H} = -J_{\text{ex}} \sum_j (\hat{\sigma}_j^+ \hat{\sigma}_{j+1}^- + \hat{\sigma}_j^- \hat{\sigma}_{j+1}^+)$, where J_{ex} is the exchange coupling, $\hat{\sigma}_j^\pm$ are spin-1/2 raising (lowering) operators acting on particle j [18, 19]. We write an infinite spin-chain state with a single up-spin impurity on site j as $|j\rangle \equiv |\dots, 0_{j-1}, 1_j, 0_{j+1}, \dots\rangle$, where $|1\rangle$ ($|0\rangle$) refers to spin up (down) states in the z -basis, and choose the initial state as $|0\rangle$, i.e. with the up-spin impurity at the center of the chain. For later times the excitation travels coherently to both sides of the chain as described by the state of the system $|\psi(t)\rangle = \sum_j \phi_j(t) |j\rangle$, where $\phi_j(t) = i^j J_j(tJ_{\text{ex}}/\hbar)$ with $J_j(x)$ the Bessel function of the first kind [20]. In the first column of fig. 2, the generation of concurrence and its spread in a wave-like fashion along the spin-chain is shown [18, 19, 21]. It is noticeable how the maximum of the concurrence propagates to neighbouring sites, moving away from the center.

We now study the entanglement in the system under FM. Assume, that with probability $1-p$, the measurement apparatus is displaced equiprobably one site to the right or left of the chain. This case is described by eq. (2) with $\mathcal{S} = \{\mathbb{1}, T, T^\dagger\}$, and $T|j\rangle = |j+1\rangle$, $p_{\mathbb{1}} = p$, $p_T = p_{T^\dagger} = (1-p)/2$. As shown in the second column of fig. 2, the entanglement still exhibits its wave-like spreading albeit with weaker intensity as compared to the unaltered dynamics. This decoherence effect of the FM is responsible for the blurry appearance of the images, which however is not homogeneous, and is most prominent among distant symmetric pairs. Observe, for instance, that the square-like structures that can be seen for the exact dynamics at $t=6$ are almost lost when the FM is applied.

We also consider the effects of CG. For this, we group the particles in disjoint sets, as in eq. (12). To respect the symmetry $j \rightarrow -j$ of the system, we group particles in sets of two ($\pm\{1, 2\}, \pm\{3, 4\}, \dots$), with \mathcal{C}_2 , and sets of four ($\pm\{1, 2, 3, 4\}, \pm\{5, 6, 7, 8\}, \dots$), with \mathcal{C}_4 , leaving particle $j=0$ unaltered. The entanglement evolution for these two cases is shown in columns c) and d) for \mathcal{C}_2 and \mathcal{C}_4 respectively. In both cases, despite the lower resolution, the entanglement wave-like propagation can still be seen, with a higher intensity for \mathcal{C}_2 than for \mathcal{C}_4 . Interestingly, entanglement seems to be suppressed more for neighboring particles than for distant, coarse-grained particles. This is appreciated in the last two columns of fig. 2, where the pattern concentrates along the diagonal.

Symmetries and spectrum of fuzzy measurements.— Understanding the symmetries of a dynamical system is crucial to understand its dynamics. For closed quantum systems, symmetries result in quantum numbers, which are extremely useful to understand and classify, for example the spectra of atoms. Open quantum systems may

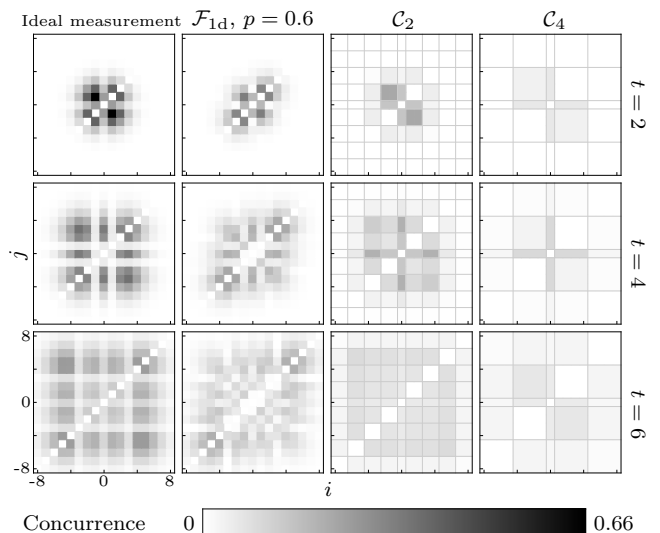


FIG. 2. Concurrence for the single spin impurity dynamics as a function of lattice sites i and j for different times. The first column shows the entanglement for the unaltered states. The second column corresponds to a FM, whereas the third and fourth columns display results for coarse grained descriptions, grouping two and four particles respectively (gridlines group the coarse grained sets of particles). The central particle has not been coarse grained in order to keep the symmetry.

also have symmetries that shape several important features [22–24], however they cannot be treated exactly the same as for closed systems [23]. Here, we calculate all symmetries of a generic FM and, as an important example, connect them with the generic invariant space.

We now turn to the characterization of FM on a system of n particles with single particle space of dimension d . We start by considering the linear superoperator $\Gamma_{l,l'}[\varrho] = \gamma_{l,l'} \varrho$, which counts how many particles in ϱ are in $|l\rangle\langle l'|$. For example, for $\varrho = |00\rangle\langle 01| = |0\rangle\langle 0| \otimes |0\rangle\langle 1|$, $\Gamma_{0,0}[\varrho] = \Gamma_{0,1}[\varrho] = \varrho$ while $\Gamma_{1,0}[\varrho] = \Gamma_{1,1}[\varrho] = 0$. Clearly, operators $\Gamma_{l,l'}$ commute among themselves. In addition, for any particle permutation, $\Gamma_{l,l'} P[\varrho] = P \Gamma_{l,l'}[\varrho]$, and therefore $[\mathcal{F}, \Gamma_{l,l'}] = 0$, and \mathcal{F} can be diagonalized in blocks \mathcal{F}_γ , each indexed by a matrix γ with $d \times d$ integers ranging from 0 to n . The subspace of physical states is the one labeled by all diagonal γ s. The number of blocks can be counted using the stars and bars theorem [25] and is given by the binomial coefficient $\binom{d^2+n-1}{n}$. Since the total number of particles is fixed, $\sum_{l,l'} \gamma_{l,l'} = n$ in all blocks.

We notice that there are some equivalent blocks. Indeed, working in the computational basis, it can be shown by explicit substitution that if $\Gamma_{l,l'}[\varrho] = \gamma_{l,l'} \varrho$, then $\Gamma_{l',l}[\varrho^T] = \gamma_{l',l} \varrho^T$, and that $(\varrho_1, \mathcal{F}[\varrho_2]) = (\varrho_1^T, \mathcal{F}[\varrho_2^T])$ for arbitrary ϱ_1 and ϱ_2 . Both identities combined lead to $\mathcal{F}_\gamma = \mathcal{F}_{\gamma^T}$ when an appropriate order of the computational basis is used. Further block equivalences fol-

low from relabeling symmetries of the levels that allow block identification. Let Q be any of the $d!$ unitary operators that relabels the elements of the computational basis [26]. Since $[Q, P] = 0, \forall P \in \mathcal{S}$, it follows that $(\rho_1, \mathcal{F}[\rho_2]) = (Q\rho_1Q', \mathcal{F}[Q\rho_2Q'])$ for arbitrary ρ_1 and ρ_2 , establishing the equivalence between the blocks $\mathcal{F}_{M(Q)\gamma M(Q)^\top}$ and \mathcal{F}_γ , with $M(Q)$ the permutation matrix of d elements associated to Q .

If $p_P > 0$ for all elements of the symmetric group in eq. (2)], the blocks \mathcal{F}_γ are irreducible, i.e. they do not contain more invariant subspaces. To prove it, notice that if all elements of the permutation group in \mathcal{F} have a positive weight, all matrix elements of \mathcal{F}_γ in the computational basis of the corresponding subspace, are strictly positive. This is a consequence of the fact that for any two of such basis elements $\rho_{1,2}$, characterized by the same γ , there exist a permutation P such that $P[\rho_1] = \rho_2$, see the Supplementary Material. Therefore the blocks \mathcal{F}_γ are irreducible, and according to the Perron-Frobenius theorem [27], each one contains only one invariant matrix. This proves the claim made at the beginning of the paragraph. Additionally this implies that for diagonal γ , the blocks \mathcal{F}_γ define *ergodic* quantum channels [28].

Examining the qubit case provides some intuition in the interpretation of the matrix γ . For qubits, γ is a 2×2 matrix whose integer, semipositive entries should add up to n . This leaves three free parameters, which we organize as follows: $\alpha = \gamma_{1,0} + \gamma_{1,1}$ and $\beta = \gamma_{0,1} + \gamma_{1,1}$ which count the number of excitations in the ket and in the bra, respectively, and $\gamma_{1,1}$. Thanks to the identification of blocks, we can always choose $\alpha, \beta, \gamma \leq n/2$, and the degeneracy δ depends on the repeated values of the entries of γ . Thus, we can write

$$\mathcal{F}^{\text{qubits}} = \bigoplus_{\alpha, \beta, \gamma_{1,1}=0}^{\lfloor n/2 \rfloor} \mathcal{F}_{(\alpha, \beta, \gamma_{1,1})}^{\oplus \delta(\gamma)}.$$

Let us discuss some features of the spectrum of FM. We start by identifying invariant operators in each block \mathcal{F}_γ . Each of those subspaces correspond to a collection of elements of the computational basis. Notice that the uniform superposition of these elements will be invariant under the action of \mathcal{F} , and thus correspond to an eigenvalue 1. For a generic FM we indeed observe exactly $C(d^2 + n - 1, n)$ ones, one for each block, confirming what we obtained using the Perron-Frobenius theorem. We also observe that changing the probability of error, while maintaining the relative probabilities of other permutations fixed, just rescales the spectrum. In other words, $\text{Spec}(p\mathbb{1} + (1-p)\mathcal{F}) = p + (1-p)\text{Spec}(\mathcal{F})$. It must also be noted that for general channels, the spectrum is complex, but comes in conjugate pairs. However, for channels involving only swaps [e.g. eq. (3) and eq. (4)] the spectrum is real as the operator is symmetric.

The spectrum for generic situations is now analyzed. To do so, we define random measuring devices character-

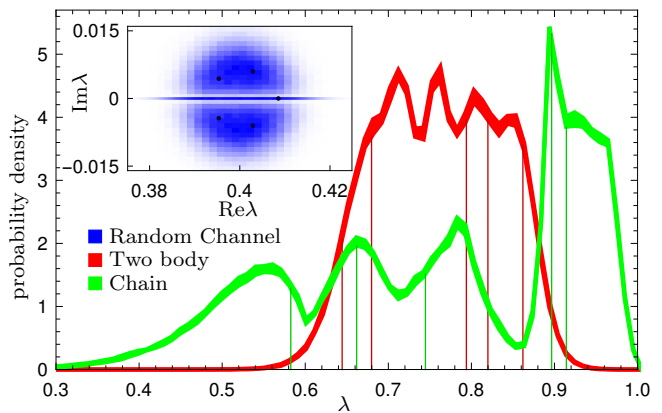


FIG. 3. Probability density of the spectrum for random FM eq. (8), 2-body eq. (3), and 1-d chains eq. (4), after removing the 1s from the invariant spaces. The calculation is done for six qubits ($n = 6, d = 2$) and the block defined by $\gamma = \text{diag}\{5, 1\}$. We studied 10^5 spectra, and for the 2-body, and 1-d chains we divided it in 10 groups to obtain a standard deviation, which is plotted as the thickness of the curves. An example of a spectrum for a single realization is also included as darker dots (inset) or lines (main figure).

ized by the channels

$$\mathcal{F}_{\text{ran}}[\rho] = p\rho + (1-p) \sum_{P \in \mathcal{S}} p_P P[\rho]. \quad (8)$$

where p describes the probability of doing the correct measurement and the p_P s are chosen uniformly and normalized such that $\sum_{P \in \mathcal{S}} p_P = 1$. We also define random 2-body and 1-dimensional FM similarly, via eq. (3) and eq. (4) respectively. For a random measuring device, \mathcal{F}_{ran} , aside from the 1s discussed above, we observe self-averaging of the eigenvalues around $1-p$, see fig. 3. This also implies a spectral gap of approximately p . For random 2-body and 1-dimensional FM there is a richer structure and, if existent, selfaveraging is much slower, see fig. 3. This might be caused by the difference in the number of terms in eq. (8) ($n!$ terms) compared with random 2-body and 1-dimensional FM with $n(n-1)/2$ and n respectively.

Invariant space of fuzzy measurements.— As mentioned above, each block contains exactly one invariant matrix. Using Theorem 1 (see Supplementary Material) it is easy to prove that for every γ , the homogeneously weighted combination of all matrix elements of \mathcal{F}_γ in the computational basis, is an invariant matrix. In fact, such invariant matrices are invariant to any permutation, according to the same theorem. Therefore, the invariant space of FM contains matrices symmetric under any permutation of the particles, and for the generic case the invariant space is such symmetric space. Furthermore its dimension can be computed using again the stars and bars theorem [25], this time for the computation of the dimension of complete symmetric tensors of tensor rank n and dimension d^2 . This immediately leads to

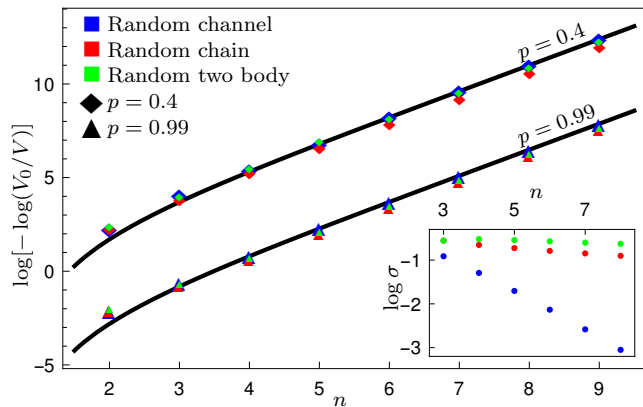


FIG. 4. We show the volume contraction of the space of density matrices under a single realization of FM for varying number of qubits, together with ansatz eq. (10). Random, 2-body and chain FM are considered, and two values for the error probability are examined. Every FM display a double exponential contraction of the state space, with respect to the number of particles. In the inset we show the standard deviation of the spectrum (ignoring the eigenvalues corresponding to the reported invariant spaces) for the aforementioned types of FM. Selfaveraging of the eigenvalues is observed only for the random general case eq. (8).

$C(d^2 + n - 1, n)$. In summary for the generic case,

$$\mathcal{F}[\Delta] = \Delta \Leftrightarrow P[\Delta] = \Delta \quad \forall P \in \mathcal{S} \quad \forall \Delta \in \mathcal{B}(\mathcal{H}). \quad (9)$$

Restricting Δ to be a hermitian positive definite operator, using Bellman inequalities, a similar result can be obtained for non-generic FMs such as \mathcal{F}_{2b} and \mathcal{F}_{1d} , see Supplementary Material. Therefore, for FM whose permutations generate the symmetric group of n particles, we identify symmetric states as the only invariant ones. This set contains of course the pure symmetric states which are simply eigenstates of the total angular momentum (being each particle a spin- $(d-1)/2$) with the maximum eigenvalue. As will be shown briefly, the set of non-symmetrical states is dramatically affected by the action of the FM.

Volume contraction.— Let us calculate the volume change when one applies a channel \mathcal{E} . For that, we consider the manifold in which density matrices live. All density matrices can be expressed as $\mathbb{1}/\text{Tr} \mathbb{1} + \sum_{i=1}^D \alpha_i G_i$ where the G_i form a traceless complete orthonormal set of matrices, say generalized Gell-Mann matrices, and $D = n^d - 1$. Treating α as a real vector in \mathbb{R}^D , we can consider the volume (with the usual measure) in such $D = n^d - 1$ space. For the qubit case this volume corresponds to the usual volume in the Bloch sphere representation. Consider now the hypercube defined by the points ρ and $\rho + \epsilon G_l$, with $l = 1, \dots, D$. The volume is $V_0 = \epsilon^D$. Under the map, the hypercube will transform to the D -parallelepiped defined by the corners $\mathcal{E}(\rho)$ and $\mathcal{E}(\rho + \epsilon G_l)$ whose signed volume is $V = V_0 \det \mathcal{E} = V_0 \prod_l \lambda_l$.

We shall calculate the volume contraction for several of the channels presented. First, consider the case of the random CG channel defined in eq. (8). Recall that the spectra has an eigenvalue of 1, degenerated $C(d^2+n-1, n)$ times. We will assume that the other eigenvalues are p , based on self-averaging and the spectral gap observed. This leads to a volume contraction given by

$$\frac{V_0}{V} \approx p \left[d^{2n} - \binom{d^2+n-1}{n} \right]. \quad (10)$$

Notice that this is a double exponential in the number of particles. In fig. 4 we show a comparison between this approximation, and a single realization of the channel, for a varying number of qubits.

This implies that exploring the space of states, even with very efficient detectors is extremely difficult. This is coherent with the difficulties found in quantum tomography [29, 30]. Fortunately, the fraction of the Hilbert space in which nature lives, seems to be quite smaller [31, 32].

Uhlmann's theorem.— We want to highlight the fact that Uhlmann's theorem can be applied to the FM scheme. Consider a hermitian matrix H , over which a probabilistic unitary conjugation is done: $G = \sum_{U \in \mathcal{U}} p_U U H U^\dagger$, with p_U probabilities adding to one, and \mathcal{U} is a finite set of unitary matrices. Then, G is majorized by H , which is denoted by $G < H$ [33]. Notice that our general FM, eq. (2), fulfills the theorem's condition. This means that $\mathcal{F}[\rho] < \rho$, which in turn means that any convex function of the density matrices will decrease under FM. Examples of convex functions include von Neumann entropy [34], a wide class of entanglement measures [35] and other quantum correlations [36].

Conclusions.— We provided a simple but powerful framework to construct coarse grained descriptions of quantum systems based on the reduction of the degrees of freedom, after the application of a FM. The latter is not only a critical step for CG, but furnishes a quantum channel scheme to address particle-indexing experimental errors. CG maps combine contributions from every particle in the system into a reduced state, effectively diminishing the number of particles and giving rise to coarser particles. Under this setting, we describe some many-body intuitive scenarios, such as sets of particles that can only be resolved by the detector as a coarser particles, and situations where such sets overlap. Fuzzy measurements, on the other hand, do not reduce the size of the system, but diminish non-symmetric correlations respect to the permutation group generated by the elements defining the FM. In fact, for the generic case the invariant space contains only symmetric operators. Using this result and the self-averaging of the spectra, we arrived to one of the central results of this letter: We showed that the volume of the accessible states contracts at a doubly exponential rate when fuzzy-like noise is present. We proved numerically that this is also the

case for the studied non-generic cases. We completed our study by applying the introduced maps to the description of entanglement waves in a spin-1/2 XX -chain. Though it is well known that in practice we cannot reconstruct the whole state of a many-body quantum system, our framework brought tools to compute the accessible state set in a wide number of scenarios.

Acknowledgments.— Support by projects CONACyT 285754 and UNAM-PAPIIT IG100518, IG101421 is acknowledged. Conversations with F. de Melo, T. H. Seligman and A. Diaz-Ruelas are also acknowledged.

Appendices

Coarse graining as FM composed with partial trace.—

In the main text we constructed a coarse graining map that describes an array of N detectors that can resolve the information of a single particle each. Assuming that each detector, labelled with k , picks at random one of m_k particles, the effective N particle state is given by

$$\rho_{\text{eff}} := \left(\bigotimes_{k=1}^N \mathcal{C}_{m_k} \right) [\rho], \quad (11)$$

$$\mathcal{C}_m[\rho] = \frac{1}{m} \text{Tr}_{\overline{1}} \sum_{i=1}^m S_{1,i}[\rho] = \text{Tr}_{\overline{1}}^{(m)} \mathcal{F}^{(m)}[\rho] \quad (12)$$

where the overline states for set complement and superscript (m) indicate that the domain of the fuzzy map and the partial trace is \mathbb{C}^{2^m} . The aim of this section is to show that it can be rewritten in the *canonical form*

$$\bigotimes_{k=1}^N \mathcal{C}_{m_k} = \text{Tr}_{\kappa} \mathcal{F}, \quad (13)$$

where \mathcal{F} and κ are a suitable choice of fuzzy map and subsystem to trace, respectively.

To find κ and \mathcal{F} we factorize the partial traces in a tensor product as their domain is disjoint,

$$\begin{aligned} \bigotimes_{k=1}^N \mathcal{C}_{m_k} &= \left(\text{Tr}_{\overline{1}}^{(1)} \otimes \dots \otimes \text{Tr}_{\overline{1}}^{(N)} \right) \left[(\mathcal{F}^{(1)} \otimes \dots \otimes \mathcal{F}^{(N)})[\rho] \right] \\ &= \text{Tr}_{\overline{\{1_1, \dots, 1_N\}}} \mathcal{F}[\rho] \end{aligned} \quad (14)$$

$$= \text{Tr}_{\kappa} \mathcal{F}, \quad (15)$$

where $1_k := 1 + \sum_{i=1}^{k-1} m_i$ is the first particle of the set S_k concerning the k th detector, defined as $S_k := \{1 + \sum_{i=1}^{k-1} m_i, \dots, \sum_{i=1}^k m_i\}$. Now let us show that $\mathcal{F} = \mathcal{F}^{(1)} \otimes \dots \otimes \mathcal{F}^{(N)}$ is a fuzzy map by distributing the tensor product,

$$\mathcal{F} = \left(\frac{1}{m_1} \sum_{i_1=1}^{m_1} S_{1,i_1} \right) \otimes \dots \otimes \left(\frac{1}{m_N} \sum_{i_N=1}^{m_N} S_{1,i_N} \right) [\rho] \quad (16)$$

$$= \prod_{j=1}^N \frac{1}{m_j} \sum_{i_1, \dots, i_N=1}^{m_1, \dots, m_N} S_{1,i_1} \otimes \dots \otimes S_{1,i_N} [\rho] \quad (17)$$

observe that \mathcal{F} is clearly a fuzzy map since tensor products of swaps result on disjoint permutations respect to particle sets.

Connection between ket-bras in \mathcal{B}_γ .— In this section we provide the connection between elements of the computational basis lying in the same invariant sector of \mathcal{F} . This result is needed to prove that sectors \mathcal{B}_γ (set of bounded operators spanned by the elements of the computational basis with matrix eigenvalue γ , see letter for further details) are irreducible for the generic case.

Theorem 1 (Connection of elements in \mathcal{B}_γ). *Let $|\bar{x}\rangle\langle\bar{y}|$, $|\bar{x}'\rangle\langle\bar{y}'| \in \mathcal{B}_\gamma$ where $|\bar{x}\rangle$, $|\bar{y}\rangle$, $|\bar{x}'\rangle$ and $|\bar{y}'\rangle$ are elements of the computational basis, and \mathcal{B}_γ is the support of \mathcal{F}_γ ; then $\exists P \in \mathcal{S}$ such that*

$$|\bar{x}'\rangle\langle\bar{y}'| = P|\bar{x}\rangle\langle\bar{y}|P^\dagger. \quad (18)$$

Proof. Let us show that every $|\bar{x}\rangle\langle\bar{y}| \in \mathcal{B}_\gamma$ can be written as a permutation of a reference ket-bra, i.e. $|\bar{x}\rangle\langle\bar{y}| = P[|\bar{x}_r^\gamma\rangle\langle\bar{y}_r^\gamma|]$, where the subscript “r” stands for *reference*. Let us now rewrite

$$|\bar{x}\rangle\langle\bar{y}| = |x_1\rangle\langle y_1| \otimes \dots \otimes |x_N\rangle\langle y_N|. \quad (19)$$

By definition, there will be $\gamma_{i,j}$ instances of the single particle operator $|i\rangle\langle j|$. One can then order the particles such that the $\gamma_{0,0}$ operators $|0\rangle\langle 0|$ are firsts, then the $\gamma_{0,1}$ operators $|0\rangle\langle 1|$ are next, and so on until the $\gamma_{d-1,d-1}$ operators $|d-1\rangle\langle d-1|$. This is the reference operator. In other words,

$$|\bar{x}_r^\gamma\rangle\langle\bar{y}_r^\gamma| = |0\rangle\langle 0|^{\otimes \gamma_{0,0}} \otimes |0\rangle\langle 1|^{\otimes \gamma_{0,1}} \otimes \dots \otimes |d-1\rangle\langle d-1|^{\otimes \gamma_{d-1,d-1}} \quad (20)$$

Such permutation will be called P . Let $|\bar{x}'\rangle\langle\bar{y}'| \in \mathcal{B}_\gamma$ be other element of the computational basis characterized by the same γ , and let P' be the corresponding permutation. Then, since

$$|\bar{x}\rangle\langle\bar{y}| = P|\bar{x}_r^\gamma\rangle\langle\bar{y}_r^\gamma|P^\dagger \quad (21)$$

$$|\bar{x}'\rangle\langle\bar{y}'| = P'|\bar{x}_r^\gamma\rangle\langle\bar{y}_r^\gamma|P'^\dagger, \quad (22)$$

we have that

$$|\bar{x}\rangle\langle\bar{y}| = P(P')^\dagger |\bar{x}'\rangle\langle\bar{y}'| P' P^\dagger \quad (23)$$

$$= P'' |\bar{x}'\rangle\langle\bar{y}'| (P'')^\dagger, \quad (24)$$

with $P'' = P(P')^\dagger$. This completes the proof. \square

Invariant states.— In the main text, using the symmetries of the generic fuzzy map and the Perron-Frobenius theorem, we have proven that a matrix Δ is invariant under generic FM if and only if it is invariant under any permutation. Here we give a theorem that holds only for hermitian positive-definite operators, but that holds for non-generic maps.

Theorem 2 (Invariant hermitian matrices). *Let Δ be a bounded positive-definite operator, and \mathcal{F} a FM defined by a probability vector \vec{p} whose non-zero entries multiply terms corresponding to a set of permutations \mathcal{A} . Then,*

$$P[\Delta] = \Delta \quad \forall P \in G_{\mathcal{A}}, \quad (25)$$

where $G_{\mathcal{A}}$ is the permutation group generated by \mathcal{A} .

Proof. Notice that if $\mathcal{F}[\Delta] = \Delta$, then $\text{Tr}[\Delta^2] = \text{Tr}[\mathcal{F}[\Delta]^2]$ holds. For density matrices this equality simply means that the purity is preserved. Developing the expression we get

$$\begin{aligned} \text{Tr}[\Delta^2] &= \text{Tr}[\mathcal{F}[\Delta]^2] \\ &= \text{Tr} \left[\left(\sum_{P \in \mathcal{A}} p_P P \Delta P^\dagger \right)^2 \right] \\ &= \sum_{P \in \mathcal{A}'} q_P \text{Tr}[P \Delta P^\dagger \Delta], \end{aligned} \quad (26)$$

where the q_P s are quadratic functions of the p_P s and \mathcal{A}' is a set of permutations generated by pairwise concatenations of elements in \mathcal{A} . Notice that the q_P s form a probability distribution. This follows from the fact that each q_P is a sum of elements of a product distribution (see the second inequality). Thus, the sum in eq. (26) is a convex combination of traces. Observe that $\mathcal{A} \subseteq \mathcal{A}'$, where the equality holds only if \mathcal{A} is a permutation group. Using the Bellman inequalities [37, 38] we have $\text{Tr}[P \Delta P^\dagger \Delta] \leq \text{Tr}[\Delta^2]$, hence the convex combination in eq. (26) equals $\text{Tr} \Delta^2$ only if $\text{Tr}[\Delta^2] = \text{Tr}[P \Delta P^\dagger \Delta]$.

Consider now the trace norm,

$$\begin{aligned} \|(\Delta - P \Delta P^\dagger)^2\|_1 &= \text{Tr} \left[\sqrt{(\Delta - P \Delta P^\dagger)^2 (\Delta - P \Delta P^\dagger)^{2\dagger}} \right] \\ &= \text{Tr} \left[(\Delta - P \Delta P^\dagger)^2 \right] \\ &= \text{Tr} \left[\Delta^2 - \Delta P \Delta P^\dagger - P \Delta P^\dagger \Delta + P \Delta^2 P^\dagger \right] \\ &= 2 \left(\text{Tr}[\Delta^2] - \text{Tr}[P \Delta P^\dagger \Delta] \right) \\ &= 0. \end{aligned}$$

The second equality follows from the hermiticity of Δ . We conclude immediately that $\|(\Delta - P \Delta P^\dagger)^2\|_1 = 0$, that from the properties of norms it follows directly $\Delta = P \Delta P^\dagger$ for all $P \in \mathcal{A}'$.

Notice that if Δ is invariant under permutations in \mathcal{A}' , then it is invariant under the permutation group generated by it, which in turn is the same group generated by \mathcal{A} , i.e. $G_{\mathcal{A}}$. \square

* carlospgmat03@gmail.com

[1] D. A. Abanin, E. Altman, I. Bloch, and M. Serbyn, Colloquium: Many-body localization, thermalization, and entanglement, *Rev. Mod. Phys.* **91**, 021001 (2019).

- [2] M. Schlosshauer, Decoherence, the measurement problem, and interpretations of quantum mechanics, *Rev. Mod. Phys.* **76**, 1267 (2005).
- [3] V. Giovannetti, S. Lloyd, and L. Maccone, Quantum metrology, *Phys. Rev. Lett.* **96**, 010401 (2006).
- [4] A. Peres, *Quantum Theory: Concepts and Methods*, Fundamental Theories of Physics (Springer Netherlands, 1995).
- [5] M. B. Mensky, Quantum restrictions for continuous observation of an oscillator, *Phys. Rev. D* **20**, 384 (1979).
- [6] S. Gudder, Non-disturbance for fuzzy quantum measurements, *Fuzzy Sets and Systems* **155**, 18 (2005).
- [7] C. Carmeli, T. Heinonen, and a. toigo, Why unsharp observables?, *Int. J. Theo. Phys.* **47**, 81 (2008).
- [8] P. Busch and G. Jaeger, Unsharp quantum reality, *Found. Phys.* **40**, 1341 (2010).
- [9] R. Quadt and P. Busch, Coarse graining and the quantum—classical connection, *Open Syst. Inf. Dyn.* **2**, 129 (1994).
- [10] J. Kofler and Č. Brukner, Classical world arising out of quantum physics under the restriction of coarse-grained measurements, *Phys. Rev. Lett.* **99**, 180403 (2007).
- [11] J. Kofler and Č. Brukner, Conditions for quantum violation of macroscopic realism, *Phys. Rev. Lett.* **101**, 090403 (2008).
- [12] C. Duarte, G. D. Carvalho, N. K. Bernardes, and F. de Melo, Emerging dynamics arising from coarse-grained quantum systems, *Phys. Rev. A* **96**, 032113 (2017).
- [13] P. Silva Correia and F. de Melo, Spin-entanglement wave in a coarse-grained optical lattice, *Phys. Rev. A* **100**, 022334 (2019).
- [14] T. Fukuhara, A. Kantian, M. Endres, M. Cheneau, P. Schauß, S. Hild, D. Bellem, U. Schollwöck, T. Giamarchi, C. Gross, I. Bloch, and S. Kuhr, Quantum dynamics of a mobile spin impurity, *Nat. Phys.* **9**, 235 (2013).
- [15] T. Fukuhara, S. Hild, J. Zeiher, P. Schauß, I. Bloch, M. Endres, and C. Gross, Spatially Resolved Detection of a Spin-Entanglement Wave in a Bose-Hubbard Chain, *Phys. Rev. Lett.* **115**, 035302 (2015).
- [16] J. F. Sherson, C. Weitenberg, M. Endres, M. Cheneau, I. Bloch, and S. Kuhr, Single-atom-resolved fluorescence imaging of an atomic Mott insulator, *Nature* **467**, 68 (2010).
- [17] W. S. Bakr, A. Peng, M. E. Tai, R. Ma, J. Simon, and 2010, Probing the superfluid-to-Mott insulator transition at the single-atom level, *Science* **239**, 547 (2010).
- [18] V. Subrahmanyam, Entanglement dynamics and quantum-state transport in spin chains, *Phys. Rev. A* **69**, 034304 (2004).
- [19] L. Amico, A. Osterloh, F. Plastina, R. Fazio, and G. M. Palma, Dynamics of entanglement in one-dimensional spin systems, *Phys. Rev. A* **69**, 022304 (2004).
- [20] N. Konno, Limit theorem for continuous-time quantum walk on the line, *Phys. Rev. E* **72**, 026113 (2005).
- [21] L. Mazza, D. Rossini, R. Fazio, and M. Endres, Detecting two-site spin-entanglement in many-body systems with local particle-number fluctuations, *New J. Phys.* **17**, 013015 (2015).
- [22] B. Buča and T. Prosen, A note on symmetry reductions of the Lindblad equation: Transport in constrained open spin chains, *New J. Phys.* **14**, 073007 (2012), arXiv:1203.0943.

- [23] D. Manzano and P. Hurtado, Harnessing symmetry to control quantum transport, *Adv. Phys.* **67**, 1 (2018), arXiv:1707.07895.
- [24] V. V. Albert and L. Jiang, Symmetries and conserved quantities in Lindblad master equations, *Phys. Rev. A* **89**, 022118 (2014), arXiv:1310.1523.
- [25] W. Feller, *An Introduction to Probability Theory and its Applications, Volume 1*, Vol. 1 (John Wiley and Sons, Inc., 1968) p. 528.
- [26] For qubits this set is $\{\mathbb{1}, \sigma_x^{\otimes n}\}$.
- [27] B. Simon, *Real Analysis* (American Mathematical Society, Providence, Rhode Island, 2015) p. 789.
- [28] D. Burgarth, G. Chiribella, V. Giovannetti, P. Perinotti, and K. Yuasa, Ergodic and mixing quantum channels in finite dimensions, *New J. Phys.* **15**, 073045 (2013), arXiv:1210.5625.
- [29] K. Banaszek, M. Cramer, and D. Gross, Focus on quantum tomography, *New J. Phys.* **15**, 125020 (2013).
- [30] S. T. Flammia, D. Gross, Y.-K. Liu, and J. Eisert, Quantum tomography via compressed sensing: error bounds, sample complexity and efficient estimators, *New J. Phys.* **14**, 095022 (2012).
- [31] R. Orús, Tensor networks for complex quantum systems, *Nature Reviews Physics* **1**, 538 (2019).
- [32] C. Pineda, T. Barthel, and J. Eisert, Unitary circuits for strongly correlated fermions, *Phys. Rev. A* **81**, 050303(R) (2010), arXiv:0905.0669.
- [33] A. Uhlmann, The “transition probability” in the state space of a $*$ -algebra, *Rep. Math. Phys.* **9**, 273 (1976).
- [34] I. Bengtsson and K. Życzkowski, *Geometry of Quantum States: An Introduction to Quantum Entanglement* (Cambridge University Press, 2017).
- [35] R. Horodecki, P. Horodecki, M. Horodecki, and K. Horodecki, Quantum entanglement, *Rev. Mod. Phys.* **81**, 865 (2009).
- [36] A. Kumar, Conditions for monogamy of quantum correlations in multipartite systems, *Phys. Lett. A* **380**, 3044 (2016).
- [37] R. Bellman, Some Inequalities for Positive Definite Matrices, in *General Inequalities 2: Proceedings of the Second International Conference on General Inequalities held in the Mathematical Research Institut at Oberwolfach, Black Forest July 30–August 5, 1978*, edited by E. F. Beckenbach (Birkhäuser Basel, Basel, 1980) pp. 89–90.
- [38] H. Zhou, On some trace inequalities for positive definite Hermitian matrices, *Journal of Inequalities and Applications* **2014**, 64 (2014).